Atmos. Chem. Phys. Discuss., 9, 19599–19640, 2009
www.atmos-chem-phys-discuss.net/9/19599/2009/

Atmospheric
Chemistry
and Physics
Discussions

Estimates of biomass burning emissions in tropical Asia based on satellite-derived data

D. Chang and Y. Song

Department of Environmental Sciences, Peking University, Beijing 100871, China

Received: 14 July 2009 – Accepted: 9 September 2009 – Published: 22 September 2009

Correspondence to: Y. Song (songyu@pku.edu.cn)

Published by Copernicus Publications on behalf of the European Geosciences Union.

Abstract

Biomass burning in tropical Asia emits large amounts of trace gases and particulate matters into the atmosphere, which has significant implications for atmospheric chemistry and climatic change. In this study, emissions from open biomass burning over tropical Asia were evaluated during seven fire years from 2000–2006 (1 April 2000–31 March 2007). Burned areas were estimated from newly published 1-km L3JRC and 500-m MODIS burned area products (MCD45A1). Available fuel loads and emission factors were assigned for each vegetation type in a GlobCover characterisation map, and fuel moisture content was taken into account when calculating combustion factors. Over the whole period, both burned areas and fire emissions clearly showed spatial and seasonal variations. The L3JRC burned areas ranged from 31 165 km^2 in fire year 2005 to 57 313 km^2 in 2000, while the MCD45A1 burned areas ranged from 54 260 km^2 in fire year 2001 to 127 068 km^2 in 2004. Comparisons of L3JRC and MCD45A1 burned areas with ground-based measurements and other satellite information were constructed in several major burning regions, and results suggested that MCD45A1 performed better in most areas than L3JRC did although with a certain degree of underestimation of burned forest areas. The average annual L3JRC-based emissions were 125, 12, 0.98, 1.91, 0.11, 0.89, 0.044, 0.022, 0.42, 3.40, and 3.68 Tg yr^{-1} for CO_2, CO, CH_4, $NMHC_s$, NO_x, NH_3, SO_2, BC, OC, $PM_{2.5}$, and PM_{10}, respectively, while MCD45A1-based emissions were 130, 9.79, 0.65, 1.14, 0.12, 0.56, 0.046, 0.036, 0.42, 3.21, and 3.49 Tg yr^{-1}. Forest burning was determined as the major source of the fire emissions due to the high carbon density. Although agricultural burning was the second important contributor, a great deal of crop residue combustion could probably be missed by satellite observations when compared to previously published data, which may be because of its small burning size. Fire emissions were mainly concentrated in Indonesia, India, Myanmar, and Cambodia. Furthermore, the peak in burned area was generally found in the early fire season, while the maximum fire emissions often occurred in the late fire season.

Title Page
Abstract | Introduction
Conclusions | References
Tables | Figures
|◀ | ▶|
◀ | ▶
Back | Close
Full Screen / Esc
Printer-friendly Version
Interactive Discussion

1 Introduction

Biomass burning is an important source of atmospheric trace gases and particulate matter, which have a significant influence on climate change and atmospheric chemistry, particularly in the tropics (Seiler and Crutzen, 1980; Hao and Liu, 1994). Fires are widely used in tropical regions for deforestation, shifting cultivation, and clearing of agricultural residue (Crutzen and Andreae, 1990; Hao et al., 1990). In the tropics, both the surface vegetation and the underlying peat constitute a large and highly concentrated carbon pool (Brown et al., 1993). Previous studies statistically evaluated the carbon released from tropical biomass burning and found that it varied between 1.8 and 4.7 Pg yr^{-1} (Seiler and Crutzen, 1980; Crutzen and Andreae, 1990; Hao et al., 1990; Hao and Liu, 1994). Recently, numerous studies evaluating fire emissions have taken advantage of satellite data products, e.g., AVHRR fire count product (Setzer and Pereira, 1991); GBA2000 product (Ito and Penner, 2004; Korontzi, 2005); VIRS fire count product and MODIS burned area dataset (Ito et al., 2007). However, many of these studies were primarily conducted in Africa and Amazonia.

Tropical Asia was considered to be the highest biomass-burning region in Asia, and has experienced some of the most severe wildland fire events under extreme climatic conditions (Chandra et al., 2002; Page et al., 2002; Streets et al., 2003). In addition, the peatland area in Southeast Asia is about 26 million ha, accounting for 69% of all tropical peatland (Rieley and Page, 2005). This peatland accumulates approximately 26–50 Gt carbon over thousands of years as a carbon sink (Page et al., 2002), a great part of which will be released to the atmosphere due to drastic land use changes, especially extensive wildfires (Shimada et al., 2000). The total amount of carbon emitted from tropical Asian biomass burning was estimated to be 238 Tg yr^{-1} in the 1990s (Streets et al., 2003), 62.8–99.7 Tg yr^{-1} in 2000 (Hoelzemann et al., 2004; Ito and Penner, 2004; Kasischke and Penner, 2004), and 420 Tg yr^{-1} from 1997–2004 (van der Werf et al., 2006). Some studies concerning biomass burning were performed in specific regions throughout tropical Asia, e.g., in Indonesia (Page et al., 2002; Langner and

Siegert, 2009), and in India (Venkataraman et al., 2006; Vadrevu et al., 2008). Streets et al. (2003) quantified the amount of emitted species from open biomass burning in Asia using published data, while Michel et al. (2005) developed an emission inventory of Asian biomass burning based on the GBA2000 algorithm. Furthermore, van der Werf et al. (2008) estimated the fire emissions in equatorial Asia between 2000 and 2006 using Measurements of Pollution in the Troposphere (MOPITT). However, these studies were either limited in time or had relatively coarse spatiotemporal resolution. Accordingly, a long-term study with relatively high resolution on the emissions from biomass burning in tropical Asia is necessary. More recently, multi-year medium spatial resolution (1 km or 500 m) and high temporal resolution global burned area products were released for public use: L3JRC product (Tansey et al., 2008), and MODIS burned area product (MCD45A1) (Roy et al., 2008). In this study, we used the two burned area products to estimate emissions (CO_2, CO, CH_4, $NMHC_s$, NO_x, NH_3, SO_2, BC, OC, $PM_{2.5}$, and PM_{10}) from open biomass burning in tropical Asia (see Fig. 1) for seven fire years from 2000–2006 (1 April 2000 to 31 March 2007).

2 Method and dataset

2.1 Method

The pollutants were mainly released from the burning of living fine and coarse tissue, fine litter, coarse woody debris (CWD), and soil organic carbon (SOC), and the method used to calculate emissions was based on the following equation described by Seiler and Crutzen (1980):

$$\text{Emission} = A \times B \times \text{CF} \times \text{EF}, \tag{1}$$

where A denotes the area burned (m^2), B is the available fuel load ($kg\,DM\,m^{-2}$), and in our study, it was represented by the biomass density, which mainly included above-ground fine and coarse fuels (live and dead) and soil organic carbon, CF (combustion factor) is the fraction of available fuels exposed to fires actually burned, and EF is the emission factor for the emitted pollutants (mass of species per mass of dry matter burned in g kg^{-1}).

The CFs and EFs are largely dependent on fuel type, moisture content, and combustion condition (Shea et al., 1996; Hoffa et al., 1999). In grassland and woodland regions, fuel moisture was taken into account in estimating CFs for fine fuels. Ito and Penner (2005) developed the relationship between CFs and the percentage of green grass out of the total grass (PGREEN), based on the measurements at eight sites in Zambia during June–September. The normalised difference vegetation index (NDVI) was used to determine PGREEN following Eq. (2) (Kogan, 1997; Burgan et al., 1998):

$$\mathrm{PGREEN}_t = (\mathrm{NDVI}_t - \mathrm{NDVI}_{\mathrm{min}})/(\mathrm{NDVI}_{\mathrm{max}} - \mathrm{NDVI}_{\mathrm{min}})\,, \tag{2}$$

where t denotes the month and $\mathrm{NDVI}_{\mathrm{min}}$ and $\mathrm{NDVI}_{\mathrm{max}}$ are the minimum and maximum of all NDVI values at a given pixel over the preceding growing season. The NDVI data were derived from the MODIS Vegetation Indices Monthly L3 Global 1 km product (MOD13A3). Missing NDVI data were replaced with the average values for the same month from the other years. For the pixels with persistently high or low NDVI values (e.g., equatorial evergreen forests or deserts), the NDVI-based method to assess PGREEN was unreliable (Korontzi, 2005). However, if these pixels were labelled as burned by the L3JRC or MCD45A1 burned area product, their PGREEN values were defined as the mean of all PGREEN values of this pixel over the whole fire year due to limited data. Previous field measurements suggested that the coarse fuels (living woody biomass and coarse woody debris) in woodland could be combusted when the CF for fine fuels was larger than 47% (Hoffa et al., 1999). Within this study, a similar CF of 0.3 was used for coarse fuels in woodland (Ito and Penner, 2004). In forested regions, defined as areas with greater than 60% tree cover, both fine fuels and coarse fuels were assumed to be burned, and the CFs of 0.90 and 0.27 were applied for the fine fuels and for coarse fuels, respectively (Ito and Penner, 2004).

EFs have been measured for multiple species in laboratories and in airborne and ground-based field studies and show strong seasonality within biomes (e.g., Shea et al., 1996; Ferek et al., 1998; Yokelson et al., 2007). In this study, we used the EFs for various compounds based on laboratory measurements of representative Indonesian fuel fires (peat, secondary forest floor litter, semak, alang-alang, and rice straw) (Christian et al., 2003). For EFs from non-agricultural fires not included in the study by Christian et al. (2003), the values from fires in Brazil were applied because the ecosystem in Brazil is more representative of the ecosystem in Indonesia (Ferek et al., 1998; Christian et al., 2003). For crop residue burning, EFs determined for developing countries were used (Yevich and Logan, 2003). When the EFs for certain emitted species were excluded in the above-mentioned publications, we used the results compiled in Andreae and Merlet (2001), which reviewed a number of studies and compiled EFs for over 100 trace gas species.

2.2 Dataset

2.2.1 Burned area

In this paper, the L3JRC burned area product and the Collection 5 MODIS (MCD45A1) burned area product were used to derive the area burned in tropical Asia from 1 April 2000 to 31 March 2007.

The L3JRC burned area product was derived from SPOT VEGETATION sensor detections that had medium spatial (1-km resolution) and high temporal resolution (daily intervals). A single algorithm was used to classify burned areas from SPOT VEGETATION reflectance data. The algorithm was successfully used over a wide geographical area and on various vegetation types, and it could be adapted for global scale application. The L3JRC product has been evaluated globally against a large number of Landsat TM and ETM+ image pairs and a number of regional products derived from in situ or remote means. Thirteen reference data sets within the Southern Asia region and Australia (below 35° N and 50° E) were reviewed, and the validation result showed that L3JRC product could only map 46.35% of the area burned (Tansey et al., 2008).

The MCD45A1 burned area product maps the location and approximate date of burning at 500-m resolution using a change detection algorithm based on a bidirectional reflectance model-based expectation method (Roy et al., 2002). This product has 8-day precision, and we allocated burns in the overlap period to the most probable calendar month to avoid potential double-counting (Roy et al., 2008). Validation of the MCD45A1 product has been performed during the 2001 fire season for 11 scenes in southern Africa, using Landsat ETM+ data (Roy and Boschetti, 2009). Results showed that the MCD45A1 product could capture 75% of the burned area detected by Landsat data. Comparison with L3JRC and GlobCarbon burned area products suggested that MCD45A1 had the highest accuracy, followed by GlobCarbon, and then by L3JRC (Roy and Boschetti, 2009).

Because L3JRC burned area product uses April as its starting month for each fire year (Tansey et al., 2008), for convenience, within our study each fire year begins on 1 April of this year and ends on 31 March of the following year.

2.2.2 Land cover characterisation

We used the European Space Agency (ESA) GlobCover land cover product (http://ionia1.esrin.esa.int/index.asp) to define the vegetation type in the studied region and to remove non-vegetated surfaces (e.g., water, snow, deserts, and urban areas) as a mask. This product is the highest-resolution (300-m) global land cover dataset presently available and covers the period during December 2004–June 2006. GlobCover is derived by automatic and regionally tuned classification of the Medium-Resolution Imaging Spectrometer (MERIS) full-resolution (FR) time series. The regional land cover product for Asia has 43 land cover classes, which are defined based on the United Nation's Land Cover Classification System (LCCS) (Bicheron et al., 2008). Within our work, the 43 vegetation classes are grouped into five broad types: forest (including broadleaf evergreen, broadleaf deciduous, needleleaf evergreen, needleleaf deciduous, and mixed forest); shrubland (including broadleaved or needleleaved, evergreen or deciduous shrubland); grassland (including close, open grassland, mosaic vegetation, sparse vegetation); cropland (including post-flooding or irrigated croplands, rainfed croplands, and mosaic cropland/vegetation); and other (including bare areas, water bodies, snow and ice, artificial surfaces and associated areas).

The MODIS Vegetation Continuous Fields product (VCF) was used to provide proportional estimates of vegetative cover types: woody vegetation, herbaceous vegetation, and bare ground. The product was derived from all seven bands of the MODIS sensor onboard NASA's Terra satellite, and had a spatial resolution of 500 m (Hansen et al., 2003). Furthermore, this dataset was overlaid onto the GlobCover vegetation characterisation map to more accurately define the land cover type in each pixel.

The World Reference Base (WRB) Map of World Soil Resources (FAO, 2003) was applied to derive the distribution of peat soils. According to the FAO soil classification, peat soils are referred to as histosols (HS), which are defined as a soil having an organic (histic) soil horizon of at least 40 cm, and the spatial distribution of peat soils in tropical Asia was illustrated in Fig. 1.

2.2.3 Fuel load

Biomass density estimates for tropical Asian forests were modelled by Brown et al. (1993) using a geographic information system. Hao and Liu (1994) and Streets et al. (2003) relied on the biomass density information from Brown et al. (1993) to estimate emissions from tropical Asian biomass burning. Ito and Penner (2004) computed the horizontal distribution of biomass density based on a tree cover data set and potential biomass density data derived by Brown et al. (1993). Brown (1997) assessed the forest biomass density for developing countries in the tropics on the basis of exiting inventories, and this estimate method was more reliable for national and global evaluations of the quantity of forest resources. In our work, the country-specific forest biomass density data for Bangladesh, Cambodia, Malaysia, Myanmar, Philippines, and Sri Lanka were taken from the results evaluated by Brown (1997), and the forest biomass information for Nepal was provided by Shrestha and Singh (2008). The district-level biomass density data in Indian forests developed by Chhabra and Dadhwal

(2004) were used, which was calculated incorporating biomass expansion factors. In addition, the biomass density values for some countries that were not included within the above publications were complemented by the data from Brown et al. (1993).

Previous studies indicated that coarse woody debris (CWD) and litterfall were the potentially significant carbon storage in the forested ecosystem, which were generally overlooked (Harmon and Hua, 1991; Matthews, 1997; Liu et al., 2003). We used the living tree biomass data utilized in our work to estimate the CWD pool based on the ratio of CWD to live tree biomass reported by Harmon and Hua (1991). They suggested that the ratio was 5% for tropical rain forests, shrublands, and grasslands, and was 20–25% for subtropical, temperate, and boreal forests (Matthews, 1997). The average litterfall densities for varied forest types at global scale compiled by Liu et al. (2003) were utilized except for India, where the district-specific estimates from Chhabra and Dadhwal (2004) were used.

The amount of biomass in the grass layer depended on local annual rainfall (Hao et al., 1990; Ito and Penner, 2004). Singh and Yadava (1974) analysed the seasonal variation in plant biomass of a tropical grassland in India and determined that the monthly aboveground biomass ranged between 0.105 kg m^{-2} in December and 1.974 kg m^{-2} in September. In our study, an average value of 0.797 kg m^{-2} was used as the mean grass biomass in India. Hashimotio et al. (2000) measured the bomass density in alang-alang grassland in Borneo during June 1993 to October 1994, and the mean value was 0.336 g m^{-2}. We used this value as the mean grass biomass density in the Indonesia and Malaysia region. Because no updated biomass density data for grass cover were available for other countries in tropical Asia, we chose an average value of 0.62 kg m^{-2}, which is also a typical dry matter density for grass loading on a global scale (Christian et al., 2003).

The amount of agricultural residue as dry matter burned in open fields was determined from crop production, the residue-to-production ratios, and the percentage of dry matter residue that was burned in the field (Yevich and Logan, 2003). The crop production data for each country were gathered from the FAO Statistical Yearbook

(FAO, 2006). For Asian countries, the percentage of agricultural residue burned in the field was reported by Yevich and Logan (2003), who also summarised the residue-to-production ratios for individual crops in developing countries. For those values that were not included in the study by Yevich and Logan (2003), we relied on the data from prior studies in Asia (Koopmans and Koppejan, 1997).

Peat combustion contributes largely to the total fire emissions in Southeast Asia, especially under El Niño conditions (Boehm et al., 2001; Page et al., 2002). However, to assess the peat quality (i.e., bulk density or carbon content) and peat burn depths is difficult and will induce significant variability in emission estimates (Shimada et al., 2000; Page et al., 2002; Ito and Penner, 2004). Brown et al. (1993) assessed the tropical Asian soil organic carbon (SOC) density based on the database of Zinke et al. (1984) and suggested a value of 14.8 kg C m^{-2} for 1 m deep. Supardi et al. (1993) gave a biomass loading value of 97.5 kg m^{-2} for dry peat of 1.5 m thickness. Batjes (1996) derived the average SOC density for different vertical depths at global scale based on World Inventory of Soil Emission Potential Database (WISE) profile dataset and the FAO Soil Map of the World. However, because they did not consider the regional differences in microclimate, parent material and land use for soils, this data was not applicable for national evaluations (Batjes, 1996). Shimada et al. (2000) estimated that the carbon density ranged from 48.7 kg C m^{-3} to 87.8 kg C m^{-3} for different peatland types in Central Kalimantan, Indonesia. Because their studies were close to our work in time and we used a mean value of 63.65 kg C m^{-3} as the SOC density in equatorial Asian peatland. The combustion efficiency in peat is often expressed in terms of the thickness of peat burned away (Heil, 2007), which varied between 20 cm and 150 cm (Boehm et al., 2001), 25 and 85 cm (Page et al., 2002) based on the field measurements in Indonesia. In our calculations, a single average peat burn depth of 51 cm was applied (Page et al., 2002).

3 Results and discussion

3.1 Burned area

Table 1 presents the burned area estimates derived from L3JRC and MCD45A1 burned area products over seven fire years from 2000–2006. The L3JRC burned areas for the seven fire years were 57 313, 44 485, 38 037, 51 977, 45 593, 31 165, and 42 575 km^2, respectively, while the MCD45A1 burned areas were 71 615, 54 260, 65 971, 102 231, 127 068, 83 579, and 92 376 km^2. On average, the latter estimates were greater than the former by a factor of 1.2 to 2.8. As shown in Fig. 2, the L3JRC burned area was mainly concentrated in central India and eastern Cambodia, while other than the extensive burning observed in India and Cambodia, the MCD45A1 product reported much more extensive burning in Myanmar and Thailand. Additionally, moderate burning was observed in the equatorial zone from the two burned area products. For L3JRC, burned area in India contributed 29 787 km^2 yr^{-1} (67.0%), followed by Myanmar 4111 km^2 yr^{-1} (9.25%), Cambodia 3236 km^2 yr^{-1} (7.28%), Nepal 2678 km^2 yr^{-1} (6.03%), Indonesia 1671 km^2 yr^{-1} (3.76%), and Thailand 1306 km^2 yr^{-1} (2.94%). For MCD45A1, the burned area occurred in India was also the largest, contributing 35 126 km^2 yr^{-1} (41.2%), followed by Myanmar 18 580 km^2 yr^{-1} (21.8%), Cambodia 12 251 km^2 yr^{-1} (14.4%), and Thailand 11 644 km^2 yr^{-1} (13.6%). Burned areas in Indonesia and Nepal only accounted for approximately 2.35% (2003 km^2 yr^{-1}) and 0.50% (430 km^2 yr^{-1}) of the total MCD45A1 burned area.

The annual estimates of the burned areas for each vegetation type are also summarised in Table 1. The average annual L3JRC burned areas for forest, shrubland, grassland, and cropland were 5855 (13.2%), 1975 (4.44%), 5604 (12.6%), and 30 179 km^2 yr^{-1} (67.9%), respectively, while the average MCD45A1 burned areas were 10 192 (11.9%), 7625 (8.94%), 8425 (9.88%), and 58 834 km^2 yr^{-1} (69.0%) for the four types. Overall, the majority of the burned area in tropical Asia occurred within cropland, followed by forest, grassland and shrubland. Large cropland burned area was related to numerous slash-and-burn agricultural and land clearing fires, especially during very dry weather conditions. However, there may be still large area of agricultural burning which was not included, because the small-sized agricultural fires were difficult to be detected by satellite sensors (Roy et al., 2008; Tansey et al., 2008). Forest fires were mostly associated with poor logging and land clearing for agricultural use in tropical regions (Crutzen and Andreae, 1990; Langner and Siegert, 2009). GBA2000 database reported a burned area of 17 000 km^2 in forest (including an unspecified part of China) for the calendar year 2000 (Ito and Penner, 2004). The MCD45A1 burned area of 10 816 km^2 in forest for fire year 2000 was more comparable to GBA2000 result than the L3JRC burned area of 8413 km^2. The large burned area reported by MCD45A1 but undetected by L3JRC was probably caused by the finer spatial resolution, cautious treatment of unclear pixels, and perhaps the burned area algorithm of MCD45A1 product. In addition, according to the peat distribution map provided by FAO (2003), an average of 676 $\mathrm{km}^2\,\mathrm{yr}^{-1}$ L3JRC burned area occurred within peat areas, while the mean burned peat area was 317 $\mathrm{km}^2\,\mathrm{yr}^{-1}$ for MCD45A1. Furthermore, nearly all of the peat burning was observed in Indonesia. It is reported that Indonesia processes about 80.4% of total peatland in Southeast Asia (Rieley and Page, 2005), and due to the damage of illegal logging and drainage, Indonesian peatland is susceptible to fires especially during El Niño period (Page et al., 2002; Langner and Siegert, 2009). Although the L3JRC and MCD45A1 burned areas in Indonesia were comparable (1671 $\mathrm{km}^2\,\mathrm{yr}^{-1}$ vs. 2003 $\mathrm{km}^2\,\mathrm{yr}^{-1}$), L3JRC reported more burning in peat areas than MCD45A1 did. However, according to the ATSR fire count data provided by RETRO inventory (REanalysis of the TROpospheric chemical composition over the past 41 years), an average of 3000 $\mathrm{km}^2\,\mathrm{yr}^{-1}$ area was burned within Indonesian peatland over 2000–2006 (Heil, 2007). Therefore, the L3JRC and MCD45A1 results may both significantly underestimate the burned peat areas.

According to Fig. 3, the peak month of L3JRC and MCD45A1 burned areas in tropical Asia was both observed during February–March. At the country level, the burned areas derived from L3JRC and MCD45A1 in India often peaked during March–May, when India experiences the high summer temperature and dry weather condition (Kiran

Chand et al., 2006). The peak burning month for Myanmar was generally in February or March, while in January or February for Cambodia. The peak month of burned area in Thailand generally occurred during January–March, which was the local dry season (www.dnp.go.th/forestfire/Eng/description.htm). Similar temporal patterns of biomass burning in these regions have also been found by a number of previous studies (e.g., Duncan et al., 2003; Tansey et al., 2004; Roy et al., 2008). As mentioned above, the sum of the burned areas in these four countries comprised 86.5% and 91.0% of the total L3JRC and MCD45A1 burned areas in tropical Asia, respectively, and apparently, the seasonal pattern of biomass burning in tropical Asia was in great part attributed to the temporal distribution of burning in these countries. It is worth noting that the peak month of L3JRC and MCD45A1 burned areas in the Indonesia and Malaysia region was observed during August–October, which was the Southern Hemisphere dry season (Duncan et al., 2003).

3.2 Comparisons of L3JRC and MCD45A1 results with independent reference data

In order to compare L3JRC and MCD45A1 burned areas with other previous estimates which were generally reported in calendar year (i.e., starting from 1 January), all L3JRC results were converted to calendar years.

3.2.1 Total burned area in tropical Asia

Total L3JRC and MCD45A1 burned areas for whole tropical Asia during calendar years 2001–2006 were first compared to the results reported in the Global Fire Emissions Database, Version 2 (GFEDv2.1) (Table 2). The GFEDv2.1 inventory was derived based on ATSR (for 1997–2000 period), TRMM-VIRS (in Africa for 1998–2000 period), and MODIS fire count data (for 2001–2006 period) (van der Werf et al., 2006). The annual L3JRC burned areas ranged from 32 713 km^2 in 2006 to 62 277 km^2 in 2001, while the annual MCD45A1 ranged from 64 708 km^2 in 2003 to 126 245 km^2 in 2004. The annual GFEDv2.1 burned areas varied between 86 282 km^2 in 2003 and 168 904 km^2 in 2004. Accordingly, the MCD45A1 and GFEDv2.1 products not only compared well with each other in the figures, but also showed a similar inter-annual variability, with the maximum burned area in 2004 and the minimum in 2003. The L3JRC results were substantially smaller than GFEDv2.1 estimates and exhibited an entirely different inter-annual change trend.

Figure 4 shows the correlation between the monthly burned areas derived in this study (i.e., L3JRC and MCD45A1 burned areas) and the GFEDv2.1 burned areas for 17 countries in tropical Asia from April 2000–December 2006. The linear regression equation and the coefficient of determination (R^2) for L3JRC and MCD45A1 are reported. It is noted that we did not include constant in equation. The regression line slope for MCD45A1 was 0.516, and the R-squared value was 0.392, while the slope and the R-squared value for L3JRC were 0.187 and 0.191, respectively. This meant that MCD45A1 was moderately correlated with GFEDv2.1 results with significant underestimation, and there was not clear relationship between L3JRC and GFEDv2.1 burned areas.

3.2.2 India

The L3JRC and MCD45A1 burned areas in India over 2001–2006 were compared to GFEDv2.1 results in Fig. 5a. L3JRC and GFEDv2.1 results were comparable in 2002 and 2006, and in other years, L3JRC showed greater burned areas than GFEDv2.1 with the differences ranging from 11 500 km^2 in 2005 to 18 182 km^2 in 2000. MCD45A1 agreed well with GFEDv2.1 burned areas in 2001, and reported significantly larger burned areas in other years with the differences ranging between 4271 km^2 in 2002 and 41 199 km^2 in 2005.

Vadrevu et al. (2008) used ATSR fire count product to characterize the spatial distribution of wildland fires in India during February–June 2006. Although the fire counts cannot determine the actual burned area, it is feasible to define the spatiotemporal pattern of vegetation fires (Vadrevu et al., 2008). The contribution of each state to the total L3JRC and MCD45A1 burned areas in India was evaluated over the period of February–June 2006, respectively, and was compared to the contribution of each state to the total ATSR fire counts during the same period (Fig. 5b). As shown, all of the three products reported significant burns in Madhya Pradesh, Maharastra, Andhra Pradesh, and Karnataka. It is worth noting that MCD45A1 showed significant overestimation of burning in Punjab and Haryana compared to L3JRC and ATSR. However, the land cover in Punjab and Haryana was dominated by agricultural regions according to GlobCover product, where the burning activities may be much more significantly missed by L3JRC and ATSR compared to MCD45A1, because of their relatively coarser resolution (van der Werf et al., 2006; Tansey et al., 2008).

The ground-based fire data in India is limited and is prone to be small in order to avoid responsibility. National statistics estimated that approximately 14 500–37 300 km^2 of forest in India were affected by fires annually (Bahuguna and Singh, 2002). Forest Survey of India (FSI) provided the extent of forest fires for 19 states since its inception. In order to compare the spatial distribution of Indian forest fires with FSI statistics, we calculated the mean annual burned forest areas derived from L3JRC and MCD45A1 for each state over the calendar years 2001–2006 (Fig. 5c). MCD45A1 and L3JRC both performed well in some regions where experienced extensive forest fires, e.g., in Madhya Pradesh, Maharashtra, Andhra Pradesh, and Orissa, and the former reported much more burned forest areas than the latter did. But in other regions with significant burning (i.e., in Uttar Pradesh, Himachal Pradesh, and Rajasthan), MCD45A1 product missed a large number of forest fires and this underestimation is probably because of the persistent cloud cover during the burning season which leads to insufficient cloud-free data available to derive the burned area algorithm (Roy et al., 2008). The better performance of L3JRC may be because of the fact that L3JRC was originally developed for boreal forest (Tansey et al., 2008).

3.2.3 Indonesia

The L3JRC and MCD45A1 burned areas in Indonesia during 2001–2006 were compared to the results developed from GFEDv2.1 data in Table 3. The L3JRC burned areas for 2001–2006 were 1084, 2526, 1281, 2285, 1182, and 2410 km^2, while the MCD45A1 burned areas were 809, 4455, 1220, 2337, 1012, and 3632 km^2, respectively. The GFEDv2.1 results were 4617, 24 180, 9410, 19 348, 24 449, and 42 300 km^2 for the six calendar years, on average 11.5 and 9.2 times larger than L3JRC and MCD45A1, respectively. As shown, a similar inter-annual variability was presented by L3JRC and MCD45A1, with two extremely extensive burning years in 2002 and 2006 which were caused by the El Niño conditions (Langner and Siegert, 2009). However, other than elevated burning detected in 2002 and 2006, GFEDv2.1 showed significant burning activity in 2005, which was the least extensive fire year during 2001–2006 according to the ATSR fire count data (Langner and Siegert, 2009). Accordingly, the GFEDv2.1 may in a certain degree overestimate the burned area in Indonesia on some occasions. RETRO biomass burning inventory showed that an average of 10 000 km^2 was burned annually in Indonesia during 2000–2006 (Heil, 2007). Therefore, both L3JRC and MCD45A1 products may significantly underestimate the burned area in the equatorial zone and need further evaluation with reliable ground observations.

3.2.4 Thailand

We compared the total burned areas in Thailand derived from L3JRC and MCD45A1 products with the GFEDv2.1 results during 2001–2006 (Table 4). As shown, the total L3JRC burned areas ranged between 479 km^2 in 2002 and 2045 km^2 in 2001, lower than the GFEDv2.1 estimates (ranging from 11 062 km^2 in 2006 to 25 957 km^2 in 2004) by a factor of 7 to 33. The MCD45A1 burned areas ranged between 6099 km^2 in 2006 and 16 412 km^2 in 2004, and matched relatively well with the GFEDv2.1 results. A comparison of the burned forest areas in Thailand obtained from different sources (Table 4) showed that L3JRC burned area for forest (110 km^2 yr^{-1}) was greatly lower than the forest fire statistics (504 km^2 yr^{-1}) provided by Forest Fire Control Division, Thailand, while the MCD45A1 burned area for forest (723 km^2 yr^{-1}) was comparable with the statistical data. Overall, MCD45A1 product performed very well in Thailand, while L3JRC showed substantial under detection of burned areas.

3.2.5 Bhutan

The total burned areas and burned forest areas in Bhutan calculated in this study were compared to GFEDv2.1 results and the statistical data compiled by IFFN (Dorji, 2006), respectively (Table 5). The annual mean L3JRC burned area was 300 km^2 yr^{-1}, significantly greater than the annual GFEDv2.1 estimate (82 km^2 yr^{-1}); while the MCD45A1 burned area was 22 km^2 yr^{-1}, smaller than GFEDv2.1 with the difference of 60 km^2. However, IFFN showed that the extents of forest fires in Bhutan for 2001–2004 were 233, 146, 57, and 26 km^2, respectively (Dorji, 2006), which were greater than the total burned areas developed from GFEDv2.1 data except for 2004. This may imply that GFEDv2.1 and MCD45A1 results underestimated the burned areas in Bhutan. The burned forest areas derived from L3JRC for 2001–2004 were 310, 229, 122, and 163 km^2, respectively, which agreed well with IFFN data. But the MCD45A1 burned areas within forest (18, 18, 5.6, and 8.5 km^2 for 2001–2004, respectively) were clearly lower than the IFFN statistics. Besides, a forest fire occurred in Wangdue district (one of the western district) in 2006–2007 record has burnt about 150 km^2 by a single case (Dorji, 2006). The burned forest area derived from L3JRC in 2006 was 204 km^2, and was 23 km^2 for MCD45A1. In consequence, L3JRC result may be more comparable to the statistical data, and MCD45A1 showed significantly underestimation in Bhutan especially within forest regions, which may be also caused by the lack of enough cloud-free data for burned area algorithm (Roy et al., 2008).

3.3 Fire emissions

The total emissions from open biomass burning for each species (CO_2, CO, CH_4, $NMHC_s$, NO_x, NH_3, SO_2, BC, OC, $PM_{2.5}$, and PM_{10}) during the seven fire years from 2000–2006 derived from the L3JRC and MCD45A1 products are presented in Table 6. The average annual L3JRC-based CO_2, CO, CH_4, $NMHC_s$, NO_x, NH_3, SO_2, BC, OC, $PM_{2.5}$, and PM_{10} emissions were 125, 12, 0.98, 1.91, 0.11, 0.89, 0.044, 0.022, 0.42, 3.40, and 3.68 Tg yr^{-1}, respectively, while the MCD45A1-based emissions were 130, 9.79, 0.65, 1.14, 0.12, 0.56, 0.046, 0.036, 0.42, 3.21, and 3.49 Tg yr^{-1}. Compared to the spatial distribution of burned areas, fire emissions from tropical Asia showed a different pattern. Indonesia was the most significant contributor to the fire emissions, followed by India, Myanmar, and Cambodia. By using CO as an illustrative example, the L3JRC-derived emissions in Indonesia, India, Myanmar, and Cambodia accounted for approximately 72.6, 13.8, 3.6, and 3.0% of the total amount, respectively, while the MCD45A1-derived emissions for these four countries comprised 42.3, 13.8, 17.6, and 10.2%. It is worth noting that 96.7% of the total L3JRC- and 95.4% of the total MCD45A1-based CO emissions in Indonesia were found in peat areas, and this highlighted the importance of soil organic carbon in biomass burning of equatorial Asia (Page et al., 2002).

The average annual emissions for several major species within forest, shrubland, grassland, and cropland are listed in Table 7, respectively. On the whole, forest was the largest contributor to fire emissions as a large carbon pool, followed by cropland, shrubland, and then by grassland. Take CO for example, the contributions of forest, cropland, shrubland, and grassland to the total L3JRC-based emission were 51.0, 25.3, 17.3, and 6.2%, respectively, and were 37.0, 31.3, 20.2, and 11.4% to the MCD45A1-based emission. However, the emissions from crop residue combustion in tropical Asia may be largely underestimated due to the fact that the agricultural fuel loading in Southeast Asia was estimated to be 4–5 kg m^{-2} (Levine, 1999; Heil, 2007), but the mean available fuel load used in this study was 0.13 kg m^{-2}. In addition, 28.1% (3.29 Tg yr^{-1}) and

71.9% (8.42 Tg yr^{-1}) of the total L3JRC-based CO emissions were attributed to aboveground vegetation and belowground SOC burning, respectively, while the contributions of the overlying vegetation and SOC to the total MCD45A1-based CO emissions were 59.6% (5.84 Tg yr^{-1}) and 40.4% (3.96 Tg yr^{-1}). As discussed in Sect. 3.1, L3JRC reported significantly larger burned area within peat areas than MCD45A1 did by a factor of 2.1, and therefore it is reasonable that the L3JRC-based emissions from peat burning were greater than MCD45A1-based emissions, which could properly explain that although total MCD45A1 burned areas were larger than L3JRC burned areas, the fire emissions derived from the two products were comparable.

The inventories of biomass burning emissions for the whole Asia that are representative of mid-1990s have been established in support of the ACE-Asia and Trace-P campaigns (Streets et al., 2003), and the emission estimates from non-agricultural and agricultural combustion for tropical Asia in this study were compared to theirs in Table 8, respectively. As shown, the emission inventories showed that CO_2, CO, CH_4, $NMHC_s$, NO_x, NH_3, SO_2, BC, and OC emissions from non-agricultural burning (including forest, shrub, and grassland fires) in tropical Asia were 573, 35, 2.06, 6.44, 1.22, 0.46, 0.21, 0.22, and 1.93 Tg yr^{-1}, respectively, which were 1–15 times higher than ours. This significant difference was mostly associated with the distinct burning data used in estimating fire emissions. The emission inventories for forest and savanna burning in tropical Asia was mostly based on the burning data from Hao and Liu (1994), which were representative of local burning information during mid-1970s and were significantly higher than the results in the recent studies (e.g., Ito and Penner, 2004). It is undoubted that the burning activities have changed drastically over last three decades (Streets et al., 2003), and consequently the discrepancy between their results and our estimates was expected. The CO_2, CO, CH_4, $NMHC_s$, NO_x, NH_3, SO_2, BC, and OC emissions from agricultural residue combustion in Streets et al. (2003) were 197, 12, 0.35, 2.04, 0.5, 0.17, 0.05, 0.09, and 0.43 Tg yr^{-1}, respectively, which were also substantially higher than those in our estimates. This may be because that their data on the amount of combusted crop residue were from the FAO statistics, which were greatly larger than those derived from burned area products in our study. As described above, the small-sized agricultural burning could not be efficiently captured by satellite sensors (Roy et al., 2008; Tansey et al., 2008). The GFEDv2.1 results showed that the total CO emissions from tropical Asian biomass burning were 248, 441, 754, 350, 744, 745, and 1116 Tg for the calendar years 2000–2006, respectively (van der Werf et al., 2006), which were 54 and 64 times L3JRC- and MCD45A1-derived CO emissions, respectively. Hoelzemann et al. (2004) calculated that 18.7 Tg of CO and 0.42 Tg of NO_x were released from Southern Asian biomass burning during calendar year 2000, respectively. However, the CO and NO_x emissions derived from L3JRC for fire year 2000 were 5.88 and 0.098 Tg, respectively, while were 5.45 and 0.096 Tg for MCD45A1. Both L3JRC- and MCD45A1-based emission estimates were significantly lower than those in previous studies. A comparison of the data used to calculate fire emissions suggested that the available fuel load values, especially the forest biomass density in our study were substantially smaller than those in previous publications (e.g., Hoelzemann et al., 2004; van der Werf et al., 2006). This may be because the literature data applied in our study only assessed the biomass density for trees above a certain diameter (Brown et al., 1993; Brown, 1997), and consequently excluded most fire susceptible parts of the vegetation (Hoelzemann et al., 2004).

3.4 Temporal variability of fire emissions

The monthly variations in CO emissions derived from the L3JRC and MCD45A1 burned area products from April 2000–March 2007 are shown in Fig. 6. Generally, there were two peaks in CO emissions, i.e., one was during February–March, and another was during August–October. The first peak was associated with aboveground vegetation fires, while the second was attributed to SOC burning. As mentioned in Sect. 3.1, the peak in burned areas often occurred in February–March, and accordingly, the seasonal distribution of emissions from overlying biomass combustion was consistent with that of burned areas. Because all peat combustion was determined in Indonesia and Malaysia region where generally experienced extensive fire activities during August–October, the fact that maximum CO emission from peat burning occurred in the late fire season was expected. Heil (2007) also stated that the contribution of peat combustion tended to rise when there were enhanced fire activities during late burning season in Indonesia owing to the intensification and prolongation of drought conditions. Ito et al. (2007) found a characteristic delay between burned areas and CO emissions in Southern Africa, and they attributed it to the increase of combustion factor as burning progressed.

4 Conclusions

In this study, emissions from open biomass burning in tropical Asia were estimated during seven fire years from 2000–2006, taking advantage of recently released satellite products: the 1-km L3JRC burned area product and 500-m MODIS product (MCD45A1). Throughout this period, the average annual L3JRC burned area was 44 449 $km^2 yr^{-1}$, while the MCD45A1 burned area was 85 300 $km^2 yr^{-1}$. For the two satellite products, the burned areas were predominantly concentrated in cropland, followed by forest, grassland and then shrubland. We compared the burned areas derived from the two products to previously published fire data for India, Indonesia, Thailand, Bhutan, and for the whole tropical Asia. Validation results suggested that the MCD45A1 product was more comparable to reference data, although underestimated the burned areas within forest; while L3JRC showed significant underestimation of the total burned areas, but may perform well in forest biomes. The average annual L3JRC-based CO_2, CO, CH_4, NO_x, BC, OC, and $PM_{2.5}$ emissions were 124.68, 11.72, 0.98, 0.11, 0.022, 0.42, and 3.40 $Tg yr^{-1}$, respectively, while MCD45A1-based emissions were 129.60, 9.79, 0.65, 0.12, 0.036, 0.42, and 3.21 $Tg yr^{-1}$. Indonesia, India, Myanmar, and Cambodia were the main contributors to fire emissions. In addition, the majority of fire emissions were attributed to forest fires, followed by cropland, shrubland, and grassland. Nevertheless, the influence of agricultural burning may be largely underestimated due to the difficulty of detecting small-sized fires by satellite sensors and the low fuel load used in this study for crop residue. The peak month of the L3JRC and MCD45A1 burned areas often occurred in February and March, while two peaks in fire emissions were observed, i.e., one was during February–March associating with aboveground vegetation burning, and another was during August–October caused by peat combustion.

Acknowledgements. The L3JRC and MCD45A1 burned area products are provided by the Joint Research Centre (JRC), European Commission, and the University of Maryland, respectively. The MODIS NDVI, VCF products are provided by the Land Process Distributed Active Archive Center (LPDAAC), USA. The GlobCover product was developed by ESA GlobCover Project, led by MEDIAS-France. This study was funded by the National Key Basic Research and Development Program of China (Grants No. 2006AA06A306).

References

Andreae, M. O. and Merlet, P.: Emission of trace gases and aerosols from biomass burning, Global Biogeochem. Cy., 15(4), 955–966, 2001.

Bahuguna, V. K. and Singh, S.: Fire situation in India, IFFN, 26, 23–27, 2002.

Batjes, N. H.: Total carbon and nitrogen in the soils of the world, Eur. J. Soil Sci., 47, 151–163, 1996.

Bicheron, P., Defourny, P., Brockmann, C., Schouten, L., Vancutsem, C., Huc, M., Bontemps, S., Leroy, M., Achard, F., Herold, M., Ranera, F., and Arino, O.: GlobCover: Products Description and Validation Report, 18, avenue E. Belin, bpi 2102, 31401 Toulouse Cedex 9, France, 2008.

Boehm, H. D. V., Siegert, F., Rieley, J. O., Page, S. E., Jauhiainen, J., Vasander, H., and Jaya, A.: Fire impacts and carbon release on tropical peatlands in Central Kalimantan, Indonesia, paper presented at the 22nd Asian Conference on Remote Sensing, Cent. For Remote Imaging, Sens., and Process., Natl. Univ. of Singapore, Singapore, 2001.

Burgan, R. E., Klaver, R. W., and Klaver, J. M.: Fuel models and fire potential from satellite and surface observations, Int. J. Wildland Fire, 8(3), 159–170, 1998.

Brown, S.: Estimating Biomass and Biomass Change of Tropical Forests, FAO For. Pap. 134, Food and Agric. Org., Rome, p. 55, 1997.

Brown, S., Iverson, L. R., Prasad, A., and Liu, D.: Geographical distributions of carbon in biomass and soils of tropical Asian forests, Geocarto Int., 4, 45–59, 1993.

Chandra, S., Ziemke, J. R., Bhartia, P. K., and Martin, R. V.: Tropical tropospheric ozone: Implications for dynamics and biomass burning, J. Geophys. Res., 107(D14), 4188, doi:10.1029/2001JD000447, 2002.

Chhabra, A. and Dadhwal, V. K.: Assessment of major pools and fluxes of carbon in Indian forests, Clim. Change, 64, 341–360, 2004.

Christian, T. J., Kleiss, B., Yokelson, R. J., Holzinger, R., Crutzen, P. J., Hao, W. M., Shirai, T., and Blake, D. R.: Comprehensive laboratory measurements of biomass-burning emissions: 1. Emissions from Indonesian, African, and other fuels, J. Geophys. Res., 108(D23), 4719, doi:10.1029/2003JD003704, 2003.

Crutzen, P. J. and Andreae, M. O.: Biomass burning in the tropics: impact on atmospheric chemistry and biogeochemical cycles, Science, 250, 1669–1678. 1990.

Dorji, T.: Fire Situation in Bhutan, IFFN, 34, 55–63, 2006.

Duncan, B. N., Martin, R. V., Staudt, A. C., Yevich, R., and Logan, J. A.: Interannual and seasonal variability of biomass burning emissions constrained by satellite observations, J. Geophys. Res.-Atmos., 108, 4100, doi:10.1029/2002JD002378, 2003.

FAO: WRB (World Reference Base) Map of World Soil Resources, Land and Water Development Division AGL, Food and Agriculture Organization of the United Nations, Rome, Italy, Available online at: http://www.fao.org/ag/agl/agll/wrb/soilres.stm (2 January 2004), 2003.

FAO: FAO Statistical Yearbook 2004, Food and Agric. Organ., Rome, 2006.

Ferek, R. J., Reid, J. S., Hobbs, P. V., Blake, D. R., and Liousse, C.: Emission factors of hydrocarbons, halocarbons, trace gases and particles from biomass burning in Brazil, J. Geophys. Res., 103(D24), 32107–32118, 1998.

Hansen, M. C., DeFries, R. S., Townshend, J. R. G., Carroll, M., Dimiceli, C., and Sohlberg, R. A.: Global percent tree cover at a spatial resolution of 500 m: First results of the MODIS vegetation continuous fields algorithm, Earth Interact., 7, 1–15, 2003.

Hao, W. M. and Liu, M. H.: Spatial and temporal distribution of tropical biomass burning, Global Biogeochem. Cy., 8, 495–503, 1994.

Hao, W. M., Liu, M. H., and Crutzen, P. J.: Estimates of annual and regional releases of CO_2 and other trace gases to the atmosphere from fires in the tropics, based on the FAO statistics for the period 1975–1980, in: Fire in the Tropical Biota: Ecosystem Processes and Global Challenges, edited by Goldammer, J. G., Ecol. Studies 84, Springer-Verlag, New York, 440–

462, 1990.

Harmon, M. E. and Hua, C.: Coarse woody debris dynamics in two old-growth, BioScience, 41(9), 604–610, 1991.

Hashimotio, T., Kojima, K., Tange, T., and Sasaki, S.: Changes in carbon storage in fallow forests in the tropical lowlands of Borneo, Forest Ecol. Manag., 126, 331–337, 2000.

Heil, A.: Indonesian forest and peat fires: emissions, air quality, and human health, Ph.D. thesis, Max Planck Inst. for Meteorol., Hamburg, 142 pp., 2007.

Hoelzemann, J. J., Schultz, M. G., Brasseur, G. P., Granier, C., and Simon, M.: Global Wildland Fire Emission Model (GWEM): Evaluating the use of global area burnt satellite data, J. Geophys. Res.-Atmos., 109, D14S04 doi:10.1029/2003JD003666, 2004.

Hoffa, E. A., Ward, D. E., Hao, W. M., Susott, R. A., and Wakimoto, R. H.: Seasonality of carbon emissions from biomass burning in a Zambian savanna, J. Geophys. Res.-Atmos., 104, 13841–13853, 1999.

Ito, A., Ito, A., and Akimoto, H.: Seasonal and interannual variations in CO and BC emissions from open biomass burning in Southern Africa during 1998–2005, Global Biogeochem. Cy., 21, GB2011, doi:10.1029/2006GB002848, 2007.

Ito, A. and Penner, J. E.: Global estimates of biomass burning emissions based on satellite imagery for the year 2000, J. Geophys. Res. Atmos., 109, D14S05, doi:10.1029/2003JD004423, 2004.

Ito, A. and Penner, J. E.: Estimates of CO emissions form open biomass burning in southern Africa for the year 2000, J. Geophys. Res., 110, D19306, doi:10.1029/2004JD005347, 2005.

Kasischke, E. S. and Penner, J. E.: Improving global estimates of atmospheric emissions from biomass burning, J. Geophys. Res.-Atmos., 109, D14S01, doi:10.1029/2004JD004972, 2004.

Kiran Chand, T. R., Badarinath, K. V. S., Krishna Prasad, V., Murthy, M. S. R., Elvidge, C. D., and Tuttle, B. T.: Monitoring forest fires over the Indian region using defense meteorological satellite program-operational Linescan system nighttime satellite data, Remote Sens. Environ., 103(2), 165–178, 2006.

Koopmans, A. and Koppejan, J.: Agricultural and Forest Residues: Generation, Utilization and Availability, Paper presented at the Regional Consultation on Modern Applications of Biomass Energy, FAO, Kuala Lumpur, Malaysia, 1997.

Kogan, F. N.: Global drought watch from space, B. Am. Meteorol. Soc., 78(4), 621–636, 1997.

Korontzi, S.: Seasonal patterns in biomass burning emissions from southern African vegetation fires for the year 2000, Global Change Biol., 11, 1680–1700, doi:10.1111/j.1365-2486.2005.01024.x, 2005.

Langner, A. and Siegert, F.: Spatiotemporal fire occurrence in Borneo over a period of 10 years, Global Change Biol., 15, 48–62, doi:10.1111/j.1365-2486.2008.01828.x, 2009.

Levine, J. S.: The 1997 fires in Kalimantan and Sumatra, Indonesia: Gaseous and particulate emissions, Geophys. Res. Lett., 26(7), 815–818, 1999.

Liu, C. J., Hannu, I., Björn, B., Werner, K., Yang, Y. S., Ma, X. Q., and Carl, J. W.: Aboveground litterfall in Eurasian forests, J. Forest. Res., 14(1), 27–34, 2003.

Matthews, E.: Global litter production, pools, and turnover times: Estimates from measurement data and regression models, J. Geophys. Res., 102(D15), 18771–18800, 1997.

Michel, C., Liousse, C., Grégoire, J. M., Tansey, K., Carmichael, G. R., and Woo, J. H.: Biomass burning emission inventory from burnt area data given by the SPOTVEGETATION system in the frame of TRACE-P and ACE-Asia campaigns, J. Geophys. Res., 110(D9), D09304, doi:10.1029/2004JD005461, 2005.

Page, S. E., Siegert, F., Rieley, J. O., Boehm, H. D. V., Jaya, A., and Limin, S.: The amount of carbon released from peat and forest fires in Indonesia during 1997, Nature, 420, 61–65, 2002.

Rieley, J. O. and Page S. E. (Eds): Wise Use of Tropical Peatlands: Focus on Southeast Asia, Alterra–Wageningen University and Research Centre and the EU INCO-STRAPEAT and RESTORPEAT Partnerships, Wageningen, The Netherlands, available at: www.restorpeat.alterra.wur.nl/download/WUG.pdf, 2005.

Roy, D. P. and Boschetti, L.: Southern Africa validation of the MODIS, L3JRC and GlobCarbon burned-area products, IEEE Geosci. Remote S., 47(4), 1032–1044, 2009.

Roy, D. P., Boschetti, L., Justice, C. O., and Ju, J.: The collection 5 MODIS burned area product-Global evaluation by comparison with the MODIS active fire product, Remote Sens. Environ., 112(9), 3690–3707, 2008.

Roy, D. P., Lewis, P., and Justice, C. O.: Burned area mapping using multi-temporal moderate spatial resolution data-A bi-directional reflectance model-based expectation approach, Remote Sens. Environ., 83, 263–286, 2002.

Seiler, W. and Crutzen, J. P.: Estimates of the gross and net fluxes of carbon between the biosphere and the atmosphere from biomass burning, Clim. Change, 2, 207–247, 1980.

Setzer, A. W. and Pereira, M. C.: Amazonia biomass burnings in 1987 and an estimate of their tropospheric emissions, Ambio, 20(1), 19–22, 1991.

Shea, R. W., Shea, B. W., Kauffman, J. B., Ward, D. E., Haskins, C. I., and Scholes, M. C.: Fuel biomass and combustion factors associated with fires in savanna ecosystems of South Africa and Zambia, J. Geophys. Res.-Atmos., 101, 23551–23568, 1996.

Shimada, S., Takahashi, H., Kaneko, M., and Haraguchi, A.: The estimation of carbon resource in a tropical peatland: a case study in Central Kalimantan, Indonesia, in: Proceedings of the International Symposium on Tropical Peatlands, edited by Iwakuma, T., et al., 22–23 Nov 1999, Bogor, Indonesia, Sapporo/Jakarta, Hokkaido University/Indonesian Institute of Sciences, 9–18, 2000.

Shrestha, B. M. and Singh, B. R.: Soil and vegetation carbon pools in a mountainous watershed of Nepal, Nutr. Cycl. Agroecosyst., 81, 179–191, 2008.

Singh, J. S. and Yadava, P. S.: Seasonal variation of composition, plant biomass, and net primary productivity of a tropical grassland at Kurukshetra, India, Ecol. Monogr., 44, 351–376, 1974.

Streets, D. G., Yarber, K. F., Woo, J.-H., and Carmichael, G. R.: Biomass burning in Asia: Annual and seasonal estimates and atmospheric emissions, Global Biogeochem. Cycles, 17(4), 1099, doi:10.1029/2003GB002040, 2003.

Supardi, A., Subekty, D., and Neuzil, S. G.: General geology and peat resources of the Siak Kanan and Bengkalis Island peat deposits, Sumatra, Indonesia, in: Modern and Ancient Coal Forming Environments, edited by: Cobb, J. C. and Cecil, C. B., Geological Society of America Special Paper, 86, 45–61, 1993.

Tansey, K., Grégoire, J. M., Binaghi, E., Boschetti, L., Brivio, P. A., Ershov, D., Flasse, S., Fraser, R., Graetz, D., Maggi, M., Peduzzi, P., Pereira, J., Silva, J., Sousa, A., and Stroppiana, D.: A global inventory of burned areas at 1 km resolution for the year 2000 derived from SPOT VEGETATION data, Clim. Change, 67, 345–377, 2004.

Tansey, K., Grégoire, J.-M., Defourny, P., Leigh, R., Pekel, J.-F., van Bogaert, E., and Bartholomé, E.: A new, global, multi-annual (2000–2007) burnt area product at 1 km resolution, Geophys. Res. Lett., 35, L01401, doi:10.1029/2007GL031567, 2008.

Vadrevu, K. P., Badarinath, K. V. S., and Anuradha, E.: Spatial patterns in vegetation fires in the Indian region, Environ. Monit. Assess., 147(1), 1–13, 2008.

van der Werf, G. R., Dempewolf, J., Trigg, S. N., Randerson, J. T., Kasibhatla, P. S., Giglio, L., Murdiyarso, D., Peters, W. Morton, D. C., Collatz, G. J., Dolman, A. J., and DeFries, R. S.: Climate regulation of fire emissions and deforestation in equatorial Asia, Proc. Natl. Acad. Sci. USA, 105, 20350–20355, 2008.

van der Werf, G. R., Randerson, J. T., Giglio, L., Collatz, G. J., Kasibhatla, P. S., and Arellano Jr., A. F.: Interannual variability in global biomass burning emissions from 1997 to 2004, Atmos. Chem. Phys., 6, 3423–3441, 2006, http://www.atmos-chem-phys.net/6/3423/2006/.

Venkataraman, C., Habib, G., Kadamba, D., Shrivastava, M., Leon, J.-F., Crouzille, B., Boucher, O., and Streets, D. G.: Emissions from open biomass burning in India: integrating the inventory approach with higher solution Moderate Resolution Imaging Spectroradiometer (MODIS) active fire and land count data, Global Biogeochem. Cy., 20, GB2013, doi:10.1029/2005GB002547, 2006.

Yevich, R. and Logan, J. A.: An assessment of biofuel use and burning of agricultural waste in the developing world, Global Biogeochem. Cy., 17(4), 1095, doi:10.1029/2002GB001 952, 2003.

Yokelson, R. J., Karl, T., Artaxo, P., Blake, D. R., Christian, T. J., Griffith, D. W. T., Guenther, A., and Hao, W. M.: The Tropical Forest and Fire Emissions Experiment: overview and airborne fire emission factor measurements, Atmos. Chem. Phys., 7, 5175–5196, 2007, http://www.atmos-chem-phys.net/7/5175/2007/.

Zinke, P. J., Stangenberger, A. G., Post, W. M., Emanuel, W. R., and Olson, J. S.: Worldwide organic soil carbon and nitrogen data, ORNL/TM-8857, Oak Ridge National Laboratory, Oak Ridge, TN, 141, 1984.

Table 1. Total burned area (km^2) derived from L3JRC and MCD45A1 burned area products during seven fire years from 2000–2006 in tropical Asia.

Fire year	2000	2001	2002	2003	2004	2005	2006	Average
				L3JRC				
Forest	8413	5566	4986	6885	5278	4392	5463	5855
Shrubland	2791	1656	1901	2490	2242	901	1847	1975
Grassland	7891	5375	4257	6687	5524	3495	5998	5604
Cropland	37 396	31 220	26 266	34 877	31 719	21 612	28 165	30 179
Other	822	668	627	1038	830	765	1102	836
Total	57 313	44 485	38 037	51 977	45 593	31 165	42 575	44 449
				MCD45A1[a]				
Forest	10 815	6830	8871	14 226	9180	8496	12 924	10 192
Shrubland	6753	4526	4488	12 917	6490	6828	11 370	7624
Grassland	8339	7005	6044	10 713	10 557	7281	9033	8425
Cropland	45 559	35 528	46 286	64 267	100 501	60 798	58 900	58 834
Other	149	371	282	107	340	176	149	225
Total	71 615	54 260	65 971	102 230	127 068	83 579	92 376	85 300

[a] MCD45A1 data for June 2001 are missing.

Table 2. Comparison of the total burned areas (km^2) derived from L3JRC and MCD45A1 products with GFEDv2.1 results during calendar years 2001–2006.

Calendar year	2001	2002	2003	2004	2005	2006	Average
L3JRC	62 277	34 188	45 618	49 759	43 047	32 713	44 601
MCD45A1[a]	67 478	71 427	64 708	126 245	114 779	76 104	86 790
GFEDv2.1	103 579	118 929	86 282	168 904	131 168	123 940	122 134

[a] MCD45A1 data for June 2001 are missing.

Table 3. Comparison of total burned areas (km^2) derived from L3JRC and MCD45A1 products in Indonesia with GFEDv2.1 results during 2001–2006.

Calendar year	2001	2002	2003	2004	2005	2006	Average
L3JRC	1084	2526	1281	2285	1182	2410	1795
MCD45A1[a]	806	4455	1220	2337	1012	3632	2244
GFEDv2.1	4617	24 180	9410	19 348	24 449	42 300	20 717

[a] MCD45A1 data for June 2001 are missing.

Table 4. Comparison of total burned areas and burned forest areas (km^2) derived from L3JRC and MCD45A1 products in Thailand with other estimates during 2001–2006[a].

Calendar year	2001	2002	2003	2004	2005	2006	Average
Total burned area							
L3JRC	2045	479	1579	1642	1301	863	1318
MCD45A1	13 825	11 201	7826	16 412	14 676	6099	11 673
GFEDv2.1	14 093	15 744	11 313	25 957	22 124	11 062	16 259
Burned forest area							
L3JRC	125	41	82	157	199	58	110
MCD45A1	725	680	221	1377	928	408	723
Statistics[b]	762	1394	158	323	303	86	504

[a] MCD45A1 data for June 2001 are missing.

[b] From Forest Fire Control Division, Thailand, available at: http://www.dnp.go.th/ForestFire/Eng/fire%20statistic.htm.

Table 5. Comparison of total burned areas and burned forest areas (km^2) derived from L3JRC and MCD45A1 products in Bhutan with other estimates during 2001–2006[a].

Calendar year	2001	2002	2003	2004	2005	2006	Average
Total burned area							
L3JRC	483	339	174	246	256	299	300
MCD45A1	37	25	7.4	16	8.0	38	22
GFEDv2.1	188	88	23	35	36	122	82
Burned forest area							
L3JRC	310	229	122	163	156	204	197
MCD45A1	18	18	5.6	8.5	4.2	23	13
Statistics[b]	233	146	57	26	–	–	116

[a] MCD45A1 data for June 2001 are missing.

[b] From International Forest Fire News (Dorji, 2006).

Table 6. Summary of fire emissions (Tg) in tropical Asia during fire years from 2000–2006.

Fire year	2000	2001	2002	2003	2004	2005	2006	Average
L3JRC								
CO_2	87.12	87.79	171.95	101.67	170.58	110.45	143.24	124.68
CO	5.88	7.47	17.99	8.31	17.47	10.88	14.02	11.72
CH_4	0.34	0.58	1.62	0.62	1.55	0.95	1.21	0.98
$NMHC_s$	0.58	1.10	3.20	1.16	3.05	1.87	2.39	1.91
NO_x	0.10	0.086	0.13	0.10	0.13	0.094	0.12	0.11
NH_3	0.27	0.51	1.51	0.54	1.44	0.87	1.11	0.89
SO_2	0.031	0.031	0.060	0.036	0.060	0.039	0.050	0.044
BC	0.027	0.019	0.021	0.024	0.023	0.017	0.022	0.022
OC	0.28	0.29	0.59	0.34	0.58	0.38	0.49	0.42
$PM_{2.5}$	1.80	2.13	5.22	2.44	5.10	3.10	4.04	3.40
PM_{10}	1.96	2.30	5.62	2.64	5.50	3.35	4.36	3.68
MCD45A1								
CO_2	91.81	70.81	193.24	140.09	162.86	87.05	161.35	129.60
CO	5.45	4.86	18.94	8.74	12.67	5.45	12.45	9.79
CH_4	0.24	0.29	1.62	0.42	0.87	0.27	0.84	0.65
$NMHC_s$	0.33	0.50	3.17	0.59	1.54	0.42	1.46	1.14
NO_x	0.10	0.068	0.15	0.14	0.15	0.10	0.15	0.12
NH_3	0.17	0.25	1.50	0.31	0.76	0.20	0.71	0.56
SO_2	0.033	0.025	0.067	0.051	0.058	0.031	0.058	0.046
BC	0.033	0.022	0.031	0.049	0.043	0.030	0.044	0.036
OC	0.29	0.22	0.66	0.44	0.51	0.27	0.52	0.42
$PM_{2.5}$	1.94	1.54	5.77	3.16	4.08	1.80	4.21	3.21
PM_{10}	2.12	1.67	6.23	3.44	4.42	1.96	4.56	3.49

Table 7. Summary of annual emissions (Tg yr^{-1}) for seven major species for each vegetation type over seven fire years from 2000–2006.

Species	CO_2	CO	CH_4	NO_x	BC	OC	$PM_{2.5}$
			L3JRC				
Forest	59.05	5.97	0.53	0.051	0.0086	0.21	1.71
Shrubland	18.72	2.03	0.18	0.014	0.0016	0.060	0.57
Grassland	11.88	0.73	0.035	0.014	0.0043	0.040	0.26
Cropland	34.46	2.96	0.23	0.029	0.0073	0.11	0.86
Other	0.58	0.025	0.0011	5.49E-04	2.00E-04	0.0017	0.0041
			MCD45A1				
Forest	44.97	3.63	0.25	0.041	0.012	0.16	1.29
Shrubland	24.09	1.98	0.14	0.022	0.005	0.06	0.56
Grassland	18.29	1.11	0.052	0.018	0.0066	0.062	0.44
Cropland	42.10	3.07	0.21	0.039	0.013	0.13	0.93
Other	0.15	0.0079	4.48E-04	2.37E-04	4.22E-05	3.87E-04	0.0012

Table 8. Comparison of the fire emissions (Tg yr^{-1}) calculated in our study with other published estimates in tropical Asia.

Species	CO_2	CO	CH_4	$NMHC_s$	NO_x	NH_3	SO_2	BC	OC
Forest/Shrub/Grassland burning									
L3JRC	89.65	8.73	0.75	1.48	0.079	0.68	0.031	0.014	0.31
MCD45A1	87.36	6.72	0.44	0.75	0.082	0.37	0.032	0.023	0.28
Streets et al. (2003)[a]	572.89	35.06	2.06	6.44	1.22	0.46	0.21	0.22	1.93
Crop residue burning									
L3JRC	34.46	2.96	0.23	0.43	0.029	0.21	0.012	0.0073	0.11
MCD45A1	42.10	3.07	0.21	0.39	0.039	0.19	0.014	0.013	0.13
Streets et al. (2003)[a]	196.61	11.94	0.35	2.04	0.50	0.17	0.052	0.090	0.43

[a] From Center for Global and Regional Environmental Research, available at: http://www.cgrer.uiowa.edu/EMISSION_DATA_new/.

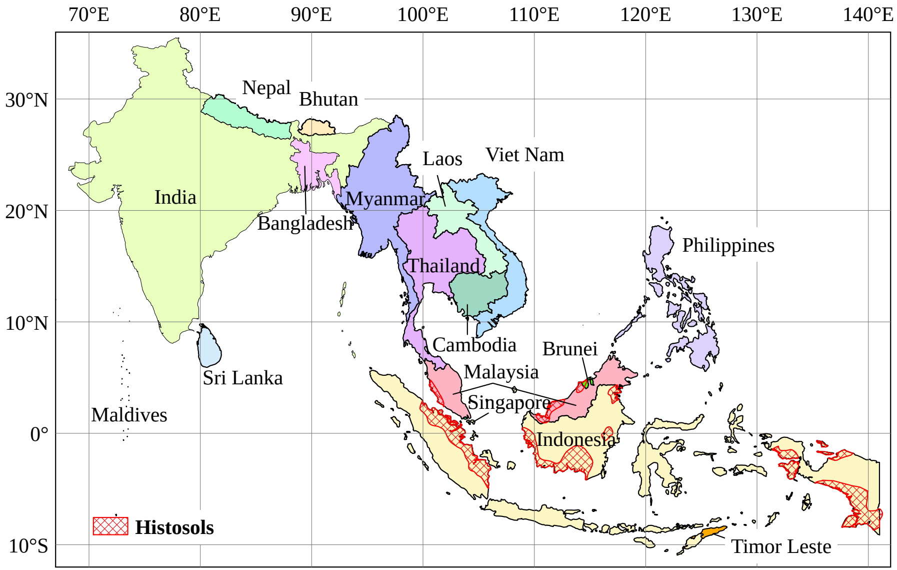

Fig. 1. Study area map and the peat distribution based on WRB map (FAO, 2003).

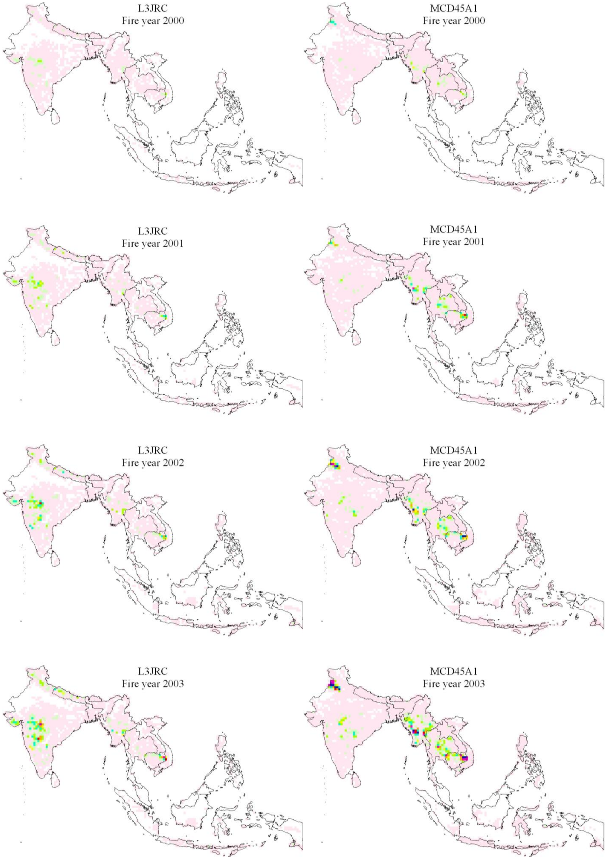

Fig. 2a. Spatial distribution of L3JRC (left) and MCD45A1 (right) burned areas in tropical Asia during seven fire years (2000–2006) (MCD45A1 data for June 2001 are lacking). Burned areas are illustrated by a color scale according to the proportion of area burned per 0.5-degree cell.

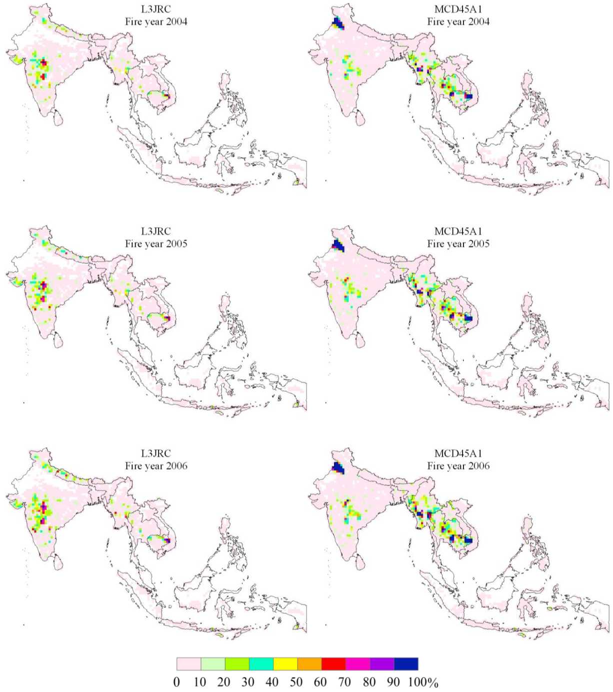

Fig. 2b. Continued.

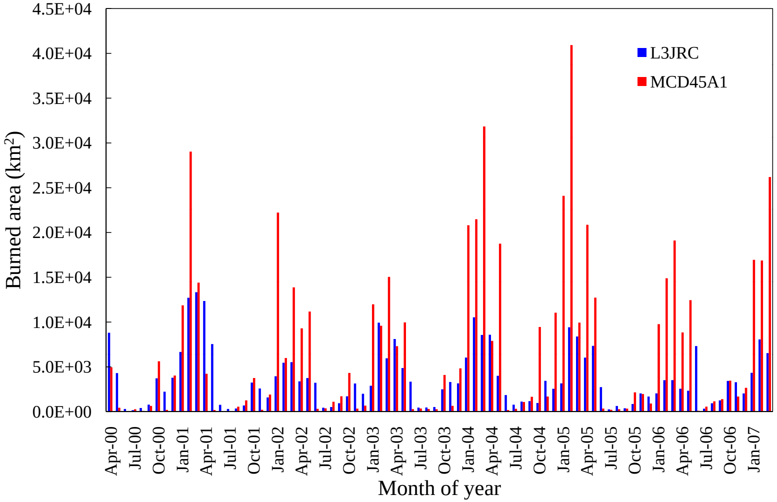

Fig. 3. Monthly L3JRC and MCD45A1 burned areas over seven fire years 2000–2006 in tropical Asia (MCD45A1 data for June 2001 are lacking).

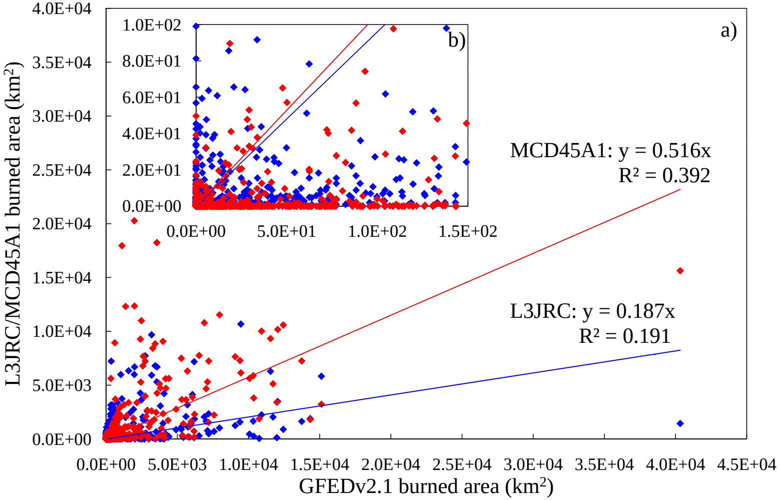

Fig. 4. Scatter plots of the monthly satellite-derived burned areas, i.e., L3JRC (blue) and MCD45A1 (red), and GFEDv2.1 estimates in tropical Asia from April 2000–December 2006 **(a)**. Small burned areas are shown in detail in **(b)**. The intercept is not included in the regression equation.

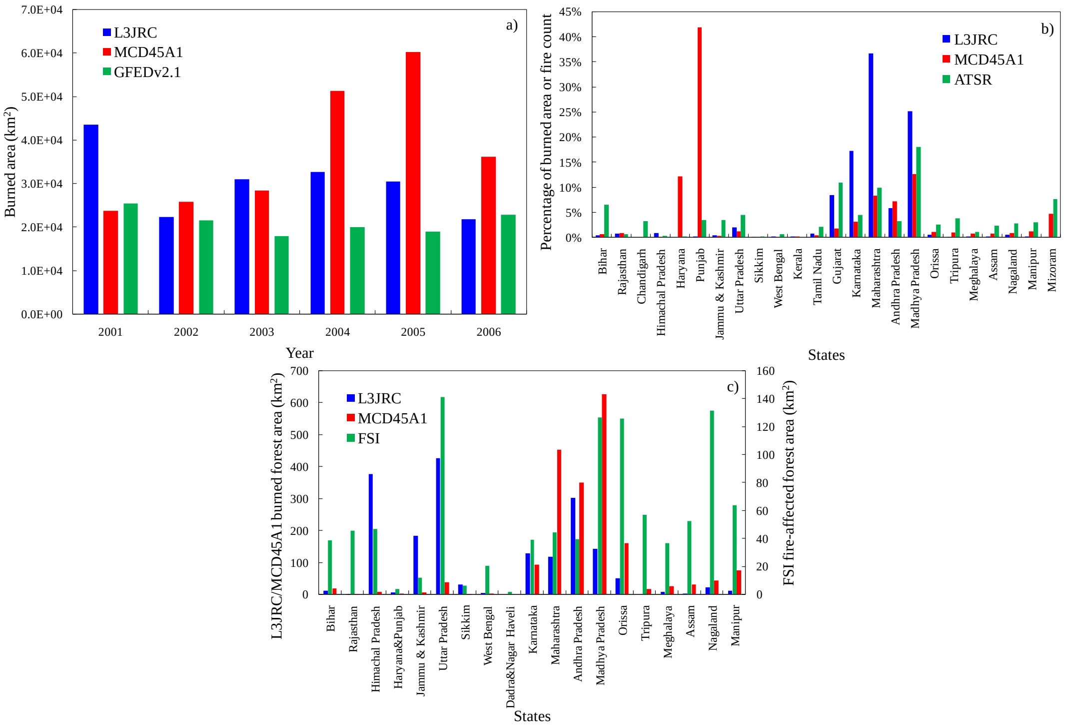

Fig. 5. (a) Comparison of total burned areas (km^2) derived from L3JRC and MCD45A1 products in India with GFEDv2.1 during 2001–2006. **(b)** Comparison of the contribution of each state to the total L3JRC and MCD45A1 burned areas and to the total ATSR fire counts over February–June 2006. **(c)** Comparison of the burned forest areas in each state derived from L3JRC and MCD45A1 with FSI statistics (Bahuguna and Singh, 2002), respectively.

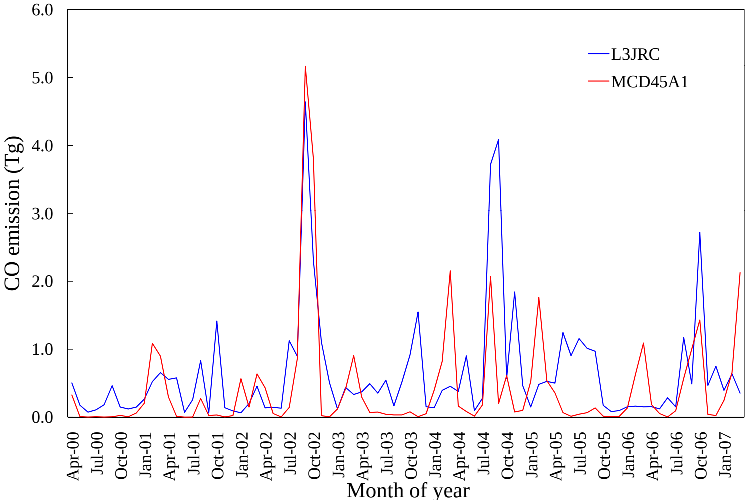

Fig. 6. Temporal distribution in CO emissions derived from L3JRC and MCD45A1 during April 2000–March 2007.